THEORETICAL AND APPLIED MECHANICS
Volume 44 (2017) Issue 2, 155–167 https://doi.org/10.2298/TAM170504007L

A PILEUP OF SCREW DISLOCATIONS AGAINST AN INCLINED BIMETALLIC INTERFACE

Vlado A. Lubarda

Dedicated to the memory of Professor Aleksandar Bakša.

Abstract. Pileups of screw dislocations against an inclined bimetallic interface are considered. It is assumed that differently oriented pileups are either under the same remote uniform loading, or under the same resolved shear stress along the pileup direction for any orientation of the interface. The distributions of dislocations and the lengths of pileups are substantially different for differently oriented interfaces, particularly in the case of the same remote loading. The interface stresses are also strongly depended on the pileup orientation. The maximum stress can be higher for a pileup along an inclined direction than along the direction orthogonal to the interface. The back stress behind a pileup is evaluated and discussed.

1. Introduction

The analysis of dislocation pileups is important for the study of the onset of plastic deformation, rate of plastic hardening, and microcracking at the grain boundaries, e.g., Eshelby et al. [1], Shilkrot and Srolovitz [2], and Anderson et al. [3]. Pileups in homeogeneous and inhomogeneous media were both considered, with and without effects of elastic anisotropy included in the analysis. Chou [4] studied a screw dislocation pileup against a rigid boundary of a semi-infinite elastic medium. Barnett [5] derived an exact solution for the distribution of screw dislocations in a pileup near a bimetallic interface by using the model of continuously distributed dislocations. Kuang and Mura [6] solved analytically the singular integral equations for the equilibrium positions of both edge and screw dislocations piled-up against a bimetallic interface. Double ended pileups of dislocations in stacked slip planes of various orientations were studied by Baskaran et al. [7] and Mesarovic et al. [8]. Dislocation pileups under non-uniform stress were considered by Liu et al. [9]. Lubarda [10,11] presented an analysis of discrete screw and edge dislocation pileups against a circular inhomogeneity and a bimaterial interface, with

2010 *Mathematics Subject Classification:* 74B99, 74L99.
Key words and phrases: back stress, bimetallic interface, dislocation pileup, screw dislocation, stress concentration.

the reference to related earlier work on the topic. An analysis of an inclined screw dislocation pileup against a welded interface between two different materials has been presented by Tucker [12] and Smith [13], who used the model of continuous distribution of infinitesimal dislocations. A pileup of screw dislocations extending from the crack tip along an inclined direction, associated with dislocation emission from the crack tip, has been studied by Chang and Mura [14]. They also used the model of continuously distributed infinitesimal dislocations, solving the corresponding mathematical problem by the extended Wiener–Hopf method.

In the present paper we consider a pileup of discrete screw dislocations along the slip direction at an arbitrary angle relative to a flat bimetallic interface. The nonlinear algebraic equations that specify equilibrium positions of dislocations are solved numerically, for a specified number of dislocations and a given shear moduli ratio G_2/G_1. Two loading scenarios are considered. The pileups are either under the same remote uniform loading, or under the same critical resolved shear stress along the pileup direction. The corresponding results for the dislocation distribution, the pileup length, and the interface and back stresses are compared and discussed. The study of edge dislocation pileups against an inclined bimetallic interface is reported separately [15].

2. Screw dislocation pileup against a bimetallic interface

An infinitely extended bimetallic block, composed of two half spaces (1) and (2) which are perfectly bonded along the interface $x = 0$ (Fig. 1), is subjected to uniform antiplane shear strain γ^0_{yz}. The remotely applied shear stress within the material (1) is then $G_1\gamma^0_{yz}$, while within the material (2) it is $G_2\gamma^0_{yz}$, where G_1 and G_2 are the respective shear moduli of two materials. The shear stresses in two materials are then uniform and given by $\sigma^{(1)}_{yz} = G_1\gamma^0_{yz}$ and $\sigma^{(2)}_{yz} = G_2\gamma^0_{yz}$, albeit discontinuous across the interface $x = 0$. There could also be a remotely applied shear stress σ^0_{xz} on the sides of the block $x = \pm\infty$, which gives rise to shear strains $\gamma^{(1)}_{xz} = \sigma^0_{xz}/G_1$, and $\gamma^{(2)}_{xz} = \sigma^0_{xz}/G_2$, with the corresponding displacement u_z continuous across the interface $x = 0$. The resolved shear stress in the z-direction over the (u, z)-plane within the material (1), where u-direction is inclined at an angle $\varphi \in [0, \pi/2)$ relative to the x-axis, is then

$$\tau^0_{nz} = \sigma^0_{yz}\cos\varphi - \sigma^0_{xz}\sin\varphi. \tag{2.1}$$

For example, if the loading is by the shear stress τ^0 only, as shown in Fig. 1, then $\sigma^0_{yz} = -\tau^0$ in the material (1), and (2.1) reduces to

$$\tau^0_{nz} = -\tau^0\cos\varphi. \tag{2.2}$$

Two loading scenarios will be considered. In the first one, τ^0 will be kept constant, so that differently oriented pileups are under different resolved shear stress $\tau^0_{nz} = -\tau^0\cos\varphi$, in accord with (2.2). In the second loading scenario, the magnitude of the resolved shear stress will be kept constant ($|\tau^0_{nz}| = \tau^{\rm cr}$) along the pileup direction for any orientation φ, so that the remote loading in this case changes with φ according to $\tau^0 = \tau^{\rm cr}/\cos\varphi$ ($\varphi \neq \pi/2$).

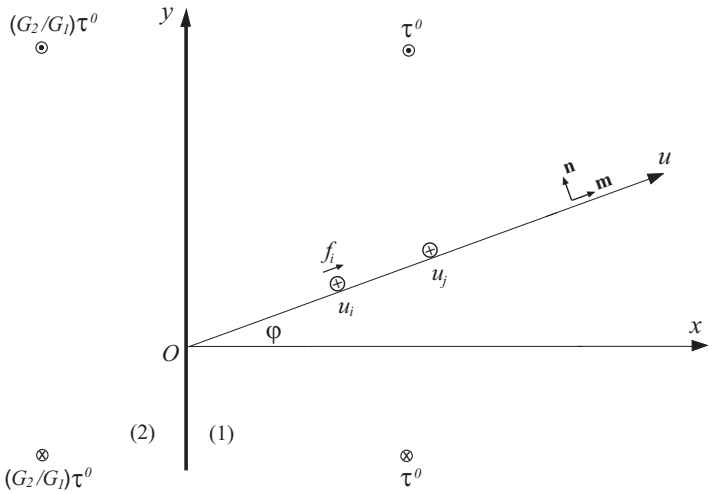

FIGURE 1. An edge dislocation at a distance u_i from a bimetallic interface along an inclined direction at an angle φ relative to x-axis orthogonal to the interface. The dislocation force from the remotely applied shear stress τ^0 and from the dislocation interaction with the interface is f_i. The unit vectors along u-direction and orthogonal to it are $(\mathbf{m}, \mathbf{n})$.

Suppose that there is a screw dislocation of a Burgers vector b_z in the material (1), at a distance u_i from the interface, along the direction u. The stress state at the point (x, y) within the material (1), produced by this dislocation, is [16, 17]

$$\begin{aligned} \sigma_{xz}^{\mathrm{disl},i}(x,y) &= -k_1 b_z \Big(\frac{y - u_i \sin\varphi}{r_i^2} + C\, \frac{y - u_i \sin\varphi}{\rho_i^2} \Big), \\ \sigma_{yz}^{\mathrm{disl},i}(x,y) &= k_1 b_z \Big(\frac{x - u_i \cos\varphi}{r_i^2} + C\, \frac{x + u_i \cos\varphi}{\rho_i^2} \Big), \end{aligned} \tag{2.3}$$

where

$$r_i^2 = (x - u_i \cos\varphi)^2 + (y - u_i \sin\varphi)^2, \quad \rho_i^2 = (x + u_i \cos\varphi)^2 + (y - u_i \sin\varphi)^2.$$

The material parameters are used

$$k_1 = \frac{G_1}{2\pi}, \quad C = \frac{G_2 - G_1}{G_2 + G_1},$$

and we assume that $G_1 < G_2 < \infty$.

The non-singular stress at the center of the dislocation $(x, y) = (u_i \cos\varphi, u_i \sin\varphi)$, from the image effects of the dislocation itself, are

$$\sigma_{xz}^{\mathrm{disl},i}(u_i) = 0, \quad \sigma_{yz}^{\mathrm{disl},i}(u_i) = k_1 b_z\, \frac{C}{2u_i \cos\varphi}, \qquad (\varphi \neq \pi/2).$$

The corresponding resolved shear stress $\tau_{nz}^{\mathrm{disl},i} = \sigma_{yz}^{\mathrm{disl},i}\cos\varphi - \sigma_{xz}^{\mathrm{disl},i}\sin\varphi$, where n is the direction orthogonal to the slip direction u (Fig. 1), is

$$\tau_{nz}^{\mathrm{disl},i}(u_i) = k_1 b_z \frac{C}{2u_i}. \tag{2.4}$$

At the point along the u-direction, at a distance $u_j \neq u_i$ from the origin at O, the coordinates $(x, y) = (u_j\cos\varphi, u_j\sin\varphi)$ and

$$r_i^2 = (u_j - u_i)^2, \quad \rho_i^2 = u_i^2 + u_j^2 + 2u_iu_j\cos 2\varphi.$$

The stress state at that point is then, from (2.3),

$$\sigma_{xz}^{\mathrm{disl},i}(u_j) = -k_1 b_z \sin\varphi\Big(\frac{1}{u_j - u_i} + C\,\frac{u_j - u_i}{u_i^2 + u_j^2 + 2u_iu_j\cos 2\varphi}\Big),$$

$$\sigma_{yz}^{\mathrm{disl},i}(u_j) = k_1 b_z \cos\varphi\Big(\frac{1}{u_j - u_i} + C\,\frac{u_j + u_i}{u_i^2 + u_j^2 + 2u_iu_j\cos 2\varphi}\Big).$$

The corresponding resolved shear stress is

$$\tau_{nz}^{\mathrm{disl},i}(u_j) = k_1 b_z\Big(\frac{1}{u_j - u_i} + C\,\frac{u_j + u_i\cos 2\varphi}{u_i^2 + u_j^2 + 2u_iu_j\cos 2\varphi}\Big). \tag{2.5}$$

3. Dislocation force on a dislocation in a pileup

If there are two dislocations, one at u_i and the other at u_j, the dislocation force on a dislocation at u_i is

$$f_i = \tau_{nz}(u_i)b_z, \quad \tau_{nz}(u_i) = \tau_{nz}^0 + \tau_{nz}^{\mathrm{disl},i}(u_i) + \tau_{nz}^{\mathrm{disl},j}(u_i).$$

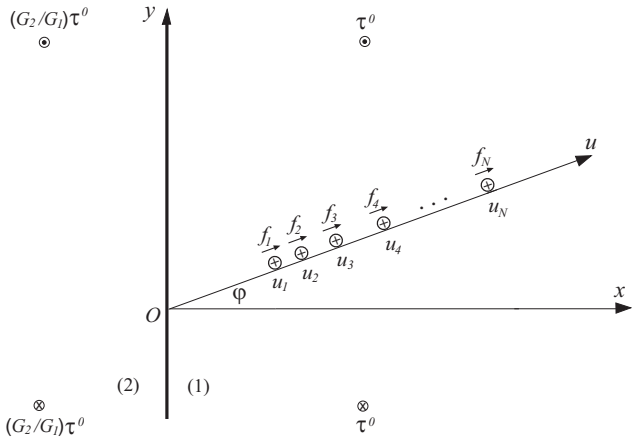

FIGURE 2. A pileup of N screw dislocations against a bimetallic interface between materials (1) and (2), which are under applied remote uniform shear stress τ^0. In the equilibrium configuration the dislocation force on each dislocation vanishes ($f_i = 0$), which specifies their equilibrium positions u_i ($i = 1, 2, \ldots, N$).

In view of (2.4) and (2.5), there follows

$$f_i = \tau^0_{nz} b_z + k_1 b_z^2 \frac{C}{2u_i} + k_1 b_z^2 \Big(\frac{1}{u_i - u_j} + C \frac{u_i + u_j \cos 2\varphi}{u_i^2 + u_j^2 + 2u_i u_j \cos 2\varphi} \Big).$$

If there are N dislocations in a pileup (Fig. 2), the total dislocation force on a dislocation at u_i is

$$f_i = \tau^0_{nz} b_z + k_1 b_z^2 \frac{C}{2u_i} + k_1 b_z^2 \sum_{j \neq i}^{N} \Big(\frac{1}{u_i - u_j} + C \frac{u_i + u_j \cos 2\varphi}{u_i^2 + u_j^2 + 2u_i u_j \cos 2\varphi} \Big).$$

If one prefers, the pileup configuration in Fig. 2 can be rotated by φ, so that the slip plane is kept horizontal while the interface is at an angle φ relative to the direction orthogonal to the slip plane.

For $\varphi = \pi/2$, a pileup is along the interface, made of N interface edge dislocations, provided that the leading dislocation in the pileup is locked. In this case, the force acting on a dislocation at y_i is

$$f_i = \tau^0_{nz} b_z + (1 + C) k_1 b_z^2 \Big[\frac{1}{y_i} + \sum_{\substack{j=2 \\ j \neq i}}^{N} \frac{1}{y_i - y_j} \Big], \quad (i = 2, 3, \dots N),$$

where y is measured from the position of the locked dislocation ($y_1 = 0$), and $1 + C = 2G_2/(G_1 + G_2)$.

4. Equilibrium positions of dislocations

In the equilibrium pileup configuration, the dislocation force on each dislocation must vanish ($f_i = 0$, $i = 1, 2, \dots, N$). This gives a system of N nonlinear algebraic equations for the equilibrium positions of dislocations

$$\frac{C}{2u_i} + \sum_{j \neq i}^{N} \Big(\frac{1}{u_i - u_j} + C \frac{u_i + u_j \cos 2\varphi}{u_i^2 + u_j^2 + 2u_i u_j \cos 2\varphi} \Big) = -\frac{\tau^0_{nz}}{k_1 b}. \tag{4.1}$$

In the first loading scenario it will be assumed that the remote uniform loading is the same for all angles φ. Thus, if the external loading is $\sigma^0_{yz} = -\tau^0$ and $\sigma^0_{xz} = 0$, the resolved shear stress is $\tau^0_{nz} = -\tau^0 \cos\varphi$ and (4.1) becomes

$$\frac{C}{2\xi_i} + \sum_{j \neq i}^{N} \Big(\frac{1}{\xi_i - \xi_j} + C \frac{\xi_i + \xi_j \cos 2\varphi}{\xi_i^2 + \xi_j^2 + 2\xi_i \xi_j \cos 2\varphi} \Big) = \cos\varphi, \quad \xi = u_i/\bar{u}. \tag{4.2}$$

The length scale $\bar{u} = k_1 b_z/\tau^0$ is conveniently used in (4.2) to cast the equilibrium conditions in a dimensionless form. In particular, if the applied shear stress is changed from τ^0 to $c\tau^0$ ($c > 0$), the equilibrium positions of dislocations change from u_i to u_i/c.

In the second loading case it will be assumed that the piling-up of dislocations occurs under the same magnitude of the resolved shear stress $|\tau^0_{nz}| = \tau^{\rm cr}$ for any orientation of the interface relative to the slip plane. The resolved shear stress is

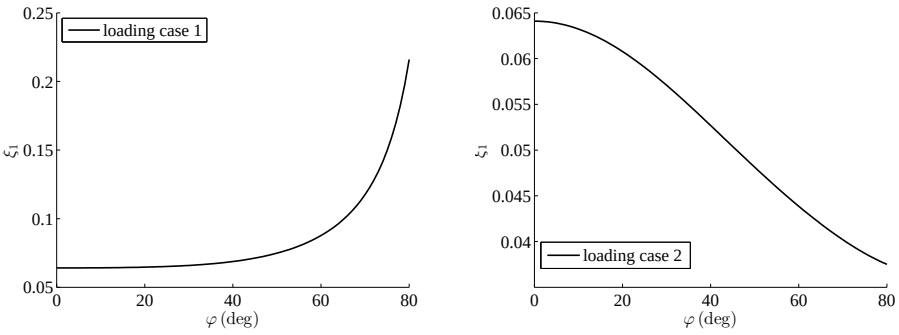

(a) (b)

FIGURE 3. The position of the leading dislocation ($\xi_1 = u_1/\bar{u}$) vs. φ in a pileup of $N = 10$ screw dislocations in the case $G_2 = 2G_1$. Part (a) is for the loading case in which τ^0 is kept constant in the expression for the resolved shear stress $\tau^0_{nz} = -\tau^0 \cos\varphi$. The corresponding length scale is $\bar{u} = k_1 b_z/\tau^0$. Part (b) is for the loading case in which $|\tau_{nz}| = \tau^{\rm cr}$ is kept constant for any φ. The remote loading in this case is $\tau^0 = \tau^{\rm cr}/\cos\varphi$, and the length scale $\bar{u} = k_1 b_z/\tau^{\rm cr}$.

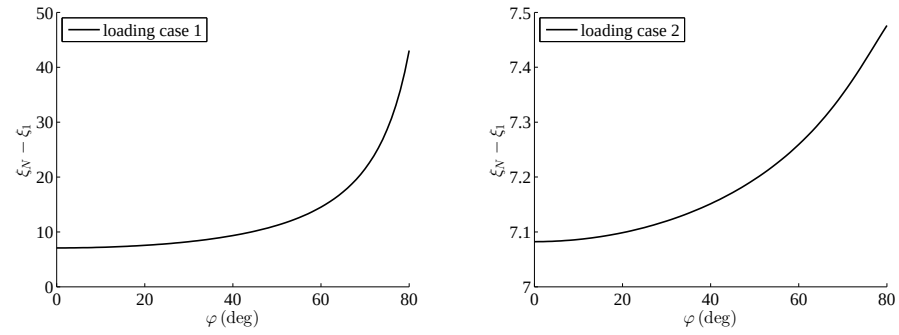

(a) (b)

FIGURE 4. The normalized length of the dislocation pileup ($\xi_N - \xi_1$) vs. φ in a pileup of $N = 10$ screw dislocations in the case $G_2 = 2G_1$. Parts (a) and (b) correspond to two loading cases described in the caption of Fig. 3.

$\tau^0_{nz} = -\tau^{\rm cr}$ to ensure the piling-up of dislocations against the repulsive forces from the interface. In this case, the equilibrium conditions (4.1) become

$$\frac{C}{2\xi_i} + \sum_{j\neq i}^{N} \Big(\frac{1}{\xi_i - \xi_j} + C\, \frac{\xi_i + \xi_j \cos 2\varphi}{\xi_i^2 + \xi_j^2 + 2\xi_i\xi_j \cos 2\varphi} \Big) = 1, \quad \xi = u_i/\bar{u},$$

with the length scale $\bar{u} = k_1 b_z/\tau^{\rm cr}$. The corresponding remote loading is different for different φ, being specified by $\tau^0 = \tau^{\rm cr}/\cos\varphi$ ($\varphi \neq \pi/2$), in accord with (2.2).

Figure 3 shows the position of the leading dislocation vs. the angle φ in a pileup of $N = 10$ dislocations in the case of material disparity $G_2 = 2G_1$. Figure 3a corresponds to the loading case 1 and Fig. 3b to the loading case 2. Figure 4 shows the corresponding pileup length, defined as the distance between the leading and the trailing dislocation of the pileup. The dependence on φ is much milder in the second loading case, in which the resolved shear stress is kept the same for all pileup orientations. Stiffer interfaces exert stronger repulsion on dislocations, so that both ξ_1 and $(\xi_N - \xi_1)$ increase with the increase of G_2/G_1.

5. Interface stresses

For the analysis of its strength it is of interest to evaluate the shear stresses along the interface. High interface stresses can cause cracking, interface relaxation by nucleation and propagation of interface dislocation, distortion of intrinsic interface dislocations, absorption of the leading dislocation, and nucleation of dislocations on the other side of the interface [18–20]. On the side of the interface toward the material (1), the shear stress components are

$$\begin{aligned}
\sigma_{xz}(0^+, y) &= -k_1 b_z (1 + C) \sum_{i=1}^{N} \frac{y - u_i \sin\varphi}{u_i^2 + y^2 - 2y u_i \sin\varphi}, \\
\sigma_{yz}(0^+, y) &= -k_1 b_z (1 - C) \sum_{i=1}^{N} \frac{u_i \cos\varphi}{u_i^2 + y^2 - 2y u_i \sin\varphi} - \tau^0.
\end{aligned} \tag{5.1}$$

The external loading is as shown in Fig. 2, i.e., $\sigma_{yz}^0 = -\tau^0$ and $\sigma_{xz}^0 = 0$.

If $(\mathbf{m}, \mathbf{n})$ are the unit vectors along the slip direction u and orthogonal to it (Fig. 1), the shear stresses with respect to these directions at the point $(x, y) = (0^+, 0)$ are

$$\begin{aligned}
\sigma_{nz}(0^+, 0) &= -k_1 b_z (1 - C\cos 2\varphi) \sum_{i=1}^{N} \frac{1}{u_i} - \tau^0 \cos\varphi, \\
\sigma_{mz}(0^+, 0) &= -k_1 b_z \sin 2\varphi \sum_{i=1}^{N} \frac{1}{u_i} - \tau^0 \sin\varphi.
\end{aligned} \tag{5.2}$$

Case 1. In the first loading case, the dimensionless forms of (5.1) and (5.2) are

$$\begin{aligned}
\hat{\sigma}_{xz}(0^+, \eta) &= -(1 + C) \sum_{i=1}^{N} \frac{\eta - \xi_i \sin\varphi}{\xi_i^2 + \eta^2 - 2\eta\xi_i \sin\varphi}, \\
\hat{\sigma}_{yz}(0^+, \eta) &= -(1 - C) \sum_{i=1}^{N} \frac{\xi_i \cos\varphi}{\xi_i^2 + \eta^2 - 2\xi_i\eta \sin\varphi} - 1,
\end{aligned}$$

and

$$\hat{\sigma}_{nz}(0^+,0) = -(1 - C\cos 2\varphi)\sum_{i=1}^{N}\frac{1}{\xi_i} - \cos\varphi,$$

$$\hat{\sigma}_{mz}(0^+,0) = -\sin 2\varphi\sum_{i=1}^{N}\frac{1}{\xi_i} - \sin\varphi,$$

where $\hat{\sigma} = \sigma/\tau^0$ for each stress component, and the lengths are normalized by $\bar{u} = k_1 b/\tau^0$, such that $\xi_i = u_i/\bar{u}$ and $\eta = y/\bar{u}$.

Case2. In the second loading case, the dimensionless forms of (5.1) and (5.2) are

$$\hat{\sigma}_{xz}(0^+,\eta) = -(1 + C)\sum_{i=1}^{N}\frac{\eta - \xi_i\sin\varphi}{\xi_i^2 + \eta^2 - 2\eta\xi_i\sin\varphi},$$

$$\hat{\sigma}_{yz}(0^+,\eta) = -(1 - C)\sum_{i=1}^{N}\frac{\xi_i\cos\varphi}{\xi_i^2 + \eta^2 - 2\xi_i\eta\sin\varphi} - \frac{1}{\cos\varphi},$$

and

$$\hat{\sigma}_{nz}(0^+,0) = -(1 - C\cos 2\varphi)\sum_{i=1}^{N}\frac{1}{\xi_i} - 1,$$

$$\hat{\sigma}_{mz}(0^+,0) = -\sin 2\varphi\sum_{i=1}^{N}\frac{1}{\xi_i} - \tan\varphi,$$

where $\hat{\sigma} = \sigma/\tau^{\rm cr}$ and the lengths are normalized by $\bar{u} = k_1 b/\tau^{\rm cr}$.

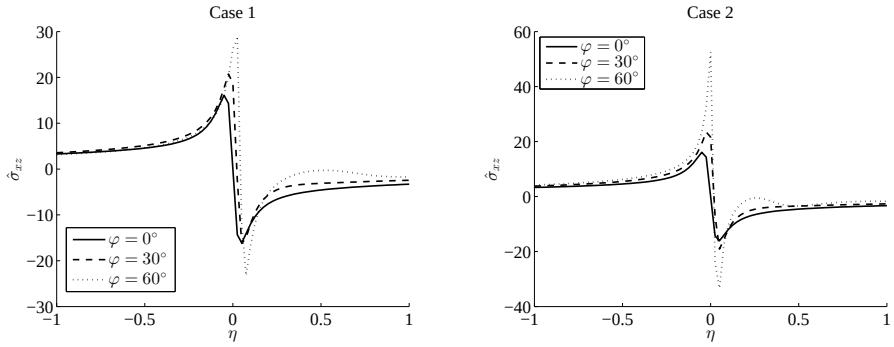

(a) (b)

FIGURE 5. The variation of the normalized shear stress $\hat{\sigma}_{xz}$ along the $\eta = y/\bar{u}$ axis on the interface side $x = 0^+$ in the case of a pileup with $N = 10$ dislocations and $G_2 = 2G_1$. Parts (a) and (b) correspond to two loading cases described in the caption of Fig. 3. In part (a) the stress is normalized by τ^0 and in part (b) by $\tau^{\rm cr}$.

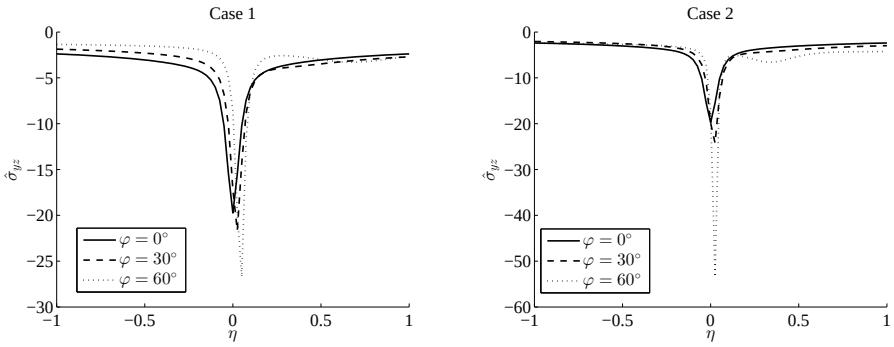

FIGURE 6. The variation of the normalized shear stress $\hat{\sigma}_{yz}$ along the $\eta = y/\bar{u}$ axis on the interface side $x = 0^+$ in the case of a pileup with $N = 10$ dislocations and $G_2 = 2G_1$. Parts (a) and (b) correspond to two loading cases described in the caption of Fig. 3.

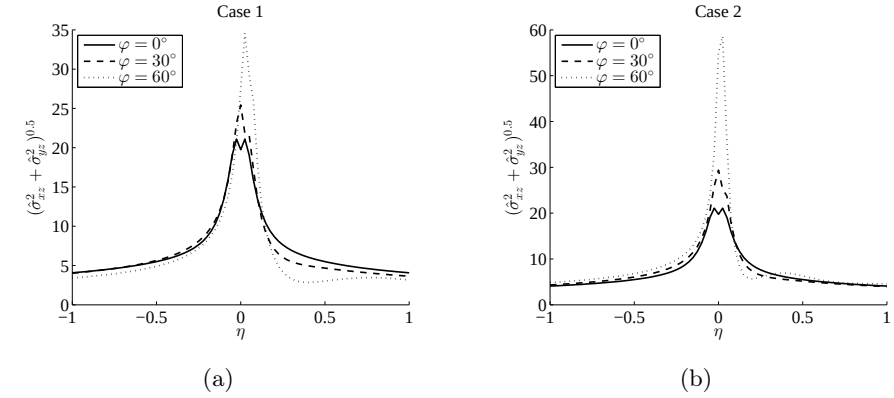

FIGURE 7. The variation of the magnitude of the total shear stress $(\hat{\sigma}_{xz}^2 + \hat{\sigma}_{yz}^2)^{1/2}$ along the η-axis corresponding to the shear stress components from Figs. 5 and 6. Parts (a) and (b) correspond to two loading cases described in the caption of Fig. 3.

The normalized interface stresses are plotted in Figures 5 and 6 for $\varphi = (0°, 30°, 60°)$. Among these values of φ, the maximum shear stress for each component occurs when $\varphi = 60°$. Figure 7 shows the variation of the corresponding total shear stress, as determined from $(\sigma_{xz}^2 + \sigma_{yz}^2)^{1/2}$, along the y-axis. The maximum shear stress is increased in the second loading case.

The variation of the normalized shear stress components $\hat{\sigma}_{nz}$ and $\hat{\sigma}_{mz}$ at the point $(x, y) = (0^+, 0)$ vs. φ is shown in Fig. 8. The pileups consist of $N = 10$ dislocations and the material disparity is $G_2 = 2G_1$.

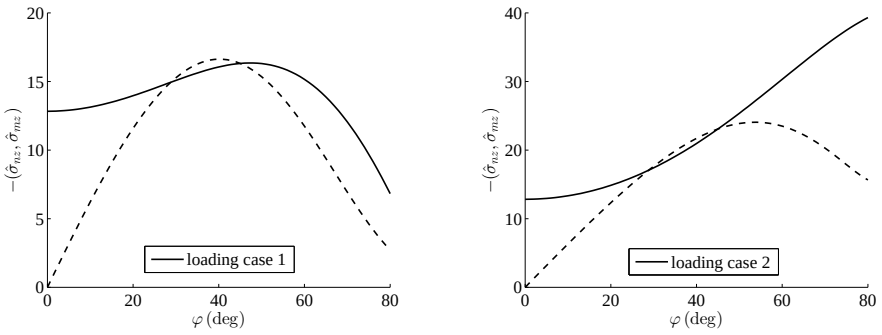

(a) (b)

FIGURE 8. The normalized shear stress components $\hat{\sigma}_{nz}$ and $\hat{\sigma}_{mz}$ at the point $(x, y) = (0^+, 0)$ vs. φ in the case of a pileup with $N = 10$ dislocations and $G_2 = 2G_1$. Parts (a) and (b) correspond to two loading cases described in the caption of Fig. 3.

6. Back stress

Piled-up dislocations exert a back stress behind a trailing dislocation of a pileup, which opposes the resolved shear stress from the applied loading and may be sufficiently large to prevent further emission of dislocations from a dislocation source within the slip plane. The back stress at any point $u > u_N$ along the slip direction, behind a trailing dislocation of the pileup (u_N), can be determined by summing up the contributions from all dislocations in the pileup. This is

$$\tau^{\rm bs} = \sum_{i=1}^{N} \tau_{nz}^{{\rm disl},i}(u), \quad \tau_{nz}^{{\rm disl},i}(u) = k_1 b_z \Big(\frac{1}{u - u_i} + C \, \frac{u + u_i \cos 2\varphi}{u^2 + u_i^2 + 2u u_i \cos 2\varphi} \Big).$$

Figure 9 shows the variation of the normalized back stress behind a trailing dislocation in the case of a pileup with $N = 10$ and $G_2 = 2G_1$, and for three selected orientation angles ($\varphi = 0°$, $30°$, and $60°$). Far behind a trailing dislocation ($u \gg u_N$), the back stress approaches the stress levels from the super-dislocation of a Burgers vector Nb_z located at the interface, which is

$$\tau^{\rm sd} = k_1(1 + C) \, \frac{N b_z}{u}.$$

In the case of a pileup in a homogeneous medium [1,3], with the leading dislocation locked, the back stress far behind a trailing dislocation is $\tau^{\rm bs} = NGb_z/(2\pi u)$, where u is the distance from the locked dislocation at $u = 0$.

7. Conclusions

We have presented in this paper an analysis of a pileup of screw dislocations against a bimetallic interface arbitrarily oriented relative to the slip plane of a

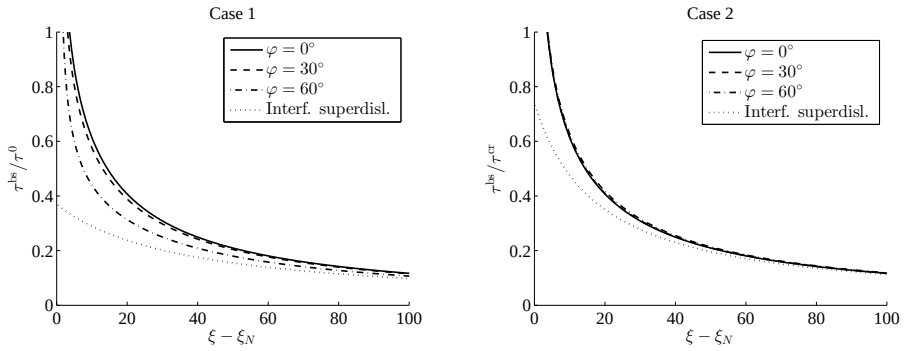

(a) (b)

FIGURE 9. (a) The variation of the normalized back stress behind a trailing dislocation ξ_N in the case of a pileup with $N = 10$ and $\Gamma = G_2/G_1 = 2$. Parts (a) and (b) correspond to two loading cases described in the caption of Fig. 3.

pileup. Two loading scenarios are considered by assuming that differently oriented pileups are either under the same remote uniform loading, or under the same resolved shear stress along the pileup direction. The equilibrium positions of dislocations are determined by solving numerically the nonlinear algebraic equations representing the conditions for the vanishing dislocation force on each dislocation from a pileup. The distributions of dislocations and the lengths of pileups are substantially different for differently oriented pileups, particularly in the case of the same remote loading. The interface stresses were found to be strongly depended on the pileup orientation. The maximum stress can be higher for a pileup along an inclined direction than along the direction orthogonal to the interface. The back stress behind a pileup is also evaluated and discussed. The obtained results may be of importance for the dislocation-based analysis of plastic deformation, including the prediction of the yield strength and the rate of plastic hardening, and the onset of microcracking at the grain boundaries of polycrystalline aggregates.

Acknowledgements. This research was supported by the Montenegrin Academy of Sciences and Arts. Discussions with Professor David M. Barnett from Stanford University and helpful comments and suggestions by an anonymous reviewer are also gratefully acknowledged.

References

1. J. D. Eshelby, F. C. Frank, F. R. N. Nabarro, *The equilibrium of linear arrays of dislocations*, Philos. Mag., VII. Ser. **42** (1951), 351–364.
2. L. E. Shilkrot, D. J. Srolovitz, *Elastic analysis of finite stiffness bimaterial interfaces: application to dislocation–interface interactions*, Acta Materialia **46** (1998), 3063–3075.
3. P. M. Anderson, J. P. Hirth, J. Lothe, *Theory of Dislocations*, 3nd ed., Cambridge Univ. Press, New York, 2017.
4. Y. T. Chou, *Linear dislocation arrays in heterogeneous materials*, Acta Metallurgica **13** (1965), 779–783.

5. D. M. Barnett, *The effect of shear modulus on the stress distribution produced by a planar array of screw dislocations near a bi-metallic interface*, Acta Metallurgica **15** (1967), 589–594.
6. J. G. Kuang, T. Mura, *Dislocation pile-up in two-phase materials*, J. Appl. Phys. **39** (1968), 109–120.
7. R. Baskaran, S. Akarapu, S. Dj. Mesarovic, H. M. Zbib, *Energies and distributions of dislocations in stacked pile-ups*, Int. J. Solids Struct. **47** (2010), 1144–1153.
8. S. Dj. Mesarovic, S. Forest, J. P. Jaric, *Size-dependent energy in crystal plasticity and continuum dislocation models*, Proc. R. Soc. Lond., Ser. A, Math. Phys. Eng. Sci. **471** (2015), p. 20140868.
9. D. Liu, Y. He, B. Zhang, L. Shen, *A continuum theory of stress gradient plasticity based on the dislocation pile-up model*, Acta Materialia **80** (2014), 350–364.
10. V. L. Lubarda, *Configurational force exerted on an inhomogeneity by a pileup of screw dislocations*, Contemp. Mater. (2017), to appear.
11. V. A. Lubarda, *An analysis of edge dislocation pileups against a circular inhomogeneity or a bimetallic interface*, Int. J. Solids Struct. (2017), to appear.
12. M. O. Tucker, *Screw dislocation pile-ups in two phase materials of finite rigidity*, J. Mech. Phys. Solids **21** (1973), 411–426.
13. E. Smith, *The piling-up of screw dislocations against a rigid inclusion*, J. Mech. Phys. Solids **21** (1973), 427–430.
14. S.-J. Chang, T. Mura, *Inclined pileup of screw dlslocations at the crack tip with a dislocation-free zone*, Int. J. Eng. Sci. **25** (1987), 561–576.
15. V. A. Lubarda, *A pileup of edge dislocations against an inclined bimetallic interface*, Mech. Mater. (2017), to appear.
16. J. Dundurs, *Elastic interactions of dislocations with inhomogeneities*, in: T. Mura (ed.), *Mathematical Theory of Dislocations*, ASME, New York, 1969, 70–115.
17. R. J. Asaro, V. A. Lubarda, *Mechanics of Solids and Materials*, Cambridge Univ. Press, Cambridge, 2006.
18. S. Poulat, B. Decamps, L. Priester, J. Thibault, *Incorporation processes of extrinsic dislocations in singular, vicinal and general grain boundaries in nickel*, Mater. Sci. Eng. A **309-310** (2001), 483–485.
19. L. Priester, *"Dislocation-interface" interaction - stress accommodation processes at interfaces*, Mater. Sci. Eng. A **309-310** (2001), 430–439.
20. E. D. Guleryuz, S. Dj. Mesarovic, *Dislocation nucleation on grain boundaries: low angle twist and asymmetric tilt boundaries*, Crystals **6** (2016), 77–88.

НАГОМИЛАВАЊЕ ЗАВОЈНИХ ДИСЛОКАЦИЈА НА НАГНУТУ МЕЂУГРАНИЧНУ ПОВРШ БИМЕТАЛА

Резиме. У раду је анализирано нагомилавање завојних дислокација на нагнуту међуграничну површ биметала. Претпостављено је да је удаљено оптерећење исто за све орјентације равни клизања у односу на међуповрш биметала, или да је смичући напон у равни клизања исти за све њене орјентације. Распоред дислокација и њихов распон су зависни од орјентације равни клизања, нарочито у случају константног удаљеног оптерећења. Концентрација напона може да буде знатно већа у случају нагомилавања дислокација у правцу који није ортогоналан на међуповрш биметала. Позадински смичући напон у равни клизања иза нагомиланих дислокација је срачунат и дискутован.

Department of NanoEngineering
University of California
San Diego
La Jolla
CA 92093-0448
USA
vlubarda@ucsd.edu

(Received 04.05.2017.)
(Revised 07.08.2017.)
(Available online 07.09.2017.)